



UMC Utrecht



Utrecht
University

Developing An Ex Vivo Tumor Slice Platform For Lipid Nanoparticle Screening

Kyra Fortuin, 5687608, Master Drug Innovation, Utrecht University

Supervisors: Mariona Estapé Senti, CDL research, University Medical Center Utrecht (UMCU).

Examiners: Prof. Raymond Schiffelers, CDL research at University Medical Center Utrecht (UMCU and Prof. Enrico Mastrobattista, Department of Pharmaceutics, Utrecht Institute for Pharmaceutical Sciences (UIPS)

Abstract

Messenger RNA (mRNA) therapeutics are rapidly emerging as a promising approach for the treatment of a wide range of diseases, including cancer. This is exemplified and reinforced by the recent clinical approval of three nucleic acid-based therapeutics. The type of delivery system plays a pivotal role in the therapeutic efficacy of mRNA-based therapeutics. Among these, lipid nanoparticles (LNPs) have emerged as a highly potential and extensively-studied delivery system. The use of precision-cut tumor slices (PCTS) presents an interesting approach for the evaluation of LNPs in a more native context, as it addresses the translational gap between *in vitro* and *in vivo* studies. We present an *ex vivo* tumor slice platform for the efficient screening of a mRNA-LNP library. Tumor slices were prepared from MC38 tumors grown in C57BL/6J mice and subsequently cultured *in vitro*. Viability and (endothelial & lymphocyte) cell populations were evaluated over a 48-hour period using a metabolic activity assay, microscopy and flow cytometry. In addition, firefly luciferase (Fluc) mRNA LNPs were generated, characterized and evaluated for efficacy using a 2D *in vitro* model and the tumor slices. The cultured slices remain viable up to 5 days with endothelial and lymphocyte populations surviving up to 48 hours. Ultimately, tumor slices can be used to successfully screen mRNA LNP libraries. This presents a versatile approach for screening LNP libraries in a reproducible manner within a biologically relevant context, paving the way for more personalized strategies, in for example, cancer therapy.

Keywords: mRNA, cancer, drug delivery, tumor, lipid nanoparticles, LNP, ex vivo models, precision-cut tumor slices, LNP library screening

Layman's summary

Cancer is a general term used for a group of diseases that occur when the cells in the body start multiplying uncontrollably and form tumors. Currently, cancer is one of the main causes of death world-wide, therefore it is very important that a proper treatment is found. The treatments that are currently used to treat patients with cancer are relatively effective, but they have a lot of downsides, such as unwanted side effects. Over the past few years, a very innovative technology has gained a lot of attention in the treatment of diseases, including cancer. This is the use of messenger RNA, a piece of genetic material that can instruct the body's own cells to produce specific proteins that can help in treating diseases. In order for the mRNA to work, it needs to be delivered to the cells using a special delivery system. This can for example be done by using tiny fat-based particles as a sort of carrier, called lipid nanoparticles. These particles are made of different types of fat and can store the mRNA in the core of the particle. The lipid nanoparticles help deliver the mRNA to the target cells, and can be adjusted in a lot of ways to make this delivery easier or better. In research, these kind of treatments are often first tested using experiments with just cells, also referred to as *in vitro* testing, to see how well they work. The cells are cultured in a laboratory and then it is checked how good these lipid nanoparticles can deliver the mRNA to the cells. However, it is also needed to test this in animals, as the *in vitro* experiments do not give enough information on how good these lipid nanoparticles would work in more complex biological settings, such as animals or humans. This so called *in vivo* testing, however would require the use of a lot of animals, which is considered not very ethical to do. Therefore, scientists have been developing methods, such as 3D culture systems, that give more relevant information than classical *in vitro* testing.

One of these approaches is the use of *ex vivo* precision-cut tumor slices. These are very thin slices prepared from tumors, that can be kept alive in an *in vitro* setting. This allows the testing of lipid nanoparticles on pieces of tissue that resemble the biological setting *in vivo*, something that is especially important for cancer research, as tumors have a very complex environment with lots of different types of cells. For our research, we have developed a method to prepare these tumor slices and keep them alive for several days. We have tested multiple lipid nanoparticles, which all had different lipid ratios, to see how well they can deliver mRNA to the cells of the slices. We have shown that these tumor slices can successfully be used to test the performance of lipid nanoparticles, and that it therefore can give valuable information without using a lot of animals.

Table of Contents

Abstract	1
Layman’s Summary	2
List of Abbreviations	4
Introduction	5
Materials and Methods	7
Cell culture.....	7
Animal tissue	7
Preparation of precision-cut tumor slices	7
Culture conditions of tumor slices	7
Microscopy	8
Histology.....	8
Immunofluorescent stainings.....	8
Viability assay	9
Identification of cell populations by flow cytometry	9
LNP preparation and characterization.....	10
Lipids.....	10
Formulation of LNPs	10
Characterization of LNPs	11
In vitro transfection efficiency in MC38 cells	11
Transfection of <i>ex vivo</i> slices	11
Results	13
The effect of culturing on <i>ex vivo</i> tumor slice viability.....	13
Quantification of cell populations present in cultured tumor slices	16
Design & Characterization of LNP libraries	17
2D <i>in vitro</i> transfection efficiency of DoE library in MC38 cells	19
Transfection of <i>ex vivo</i> tumor slices	20
Discussion	22
Conclusions	25
Acknowledgements	26
References	27
Supplementary Figures	29

List of Abbreviations

BLI	Bioluminescence Imaging
CCLR	Cell Culture Lysis Reagent
DAPI	4',6-diamidino-2-phenylindole
DLS	Dynamic Light Scattering
DMEM	Dulbecco's Modified Eagle Medium
DoE	Design of Experiments
FBS	Fetal bovine serum
FFPE	Formalin-fixed, paraffin-embedded
Fluc	Firefly luciferase
H&E	hematoxylin and eosin
hATTR	transthyretin-mediated amyloidosis
HEPES	4-(2-hydroxyethyl)-1-piperazineethanesulfonic acid
IL	Ionizable lipid
LNP	Lipid nanoparticle
mRNA	Messenger RNA
NEAA	Non-essential amino acids
P/S	Penicillin/Streptomycin
PBS	Phosphate buffered Saline
PCTS	Precision-cut tumor slices
PDI	Polydispersity index
PEG	Polyethylene glycol
PFA	Paraformaldehyde
RT	Room temperature
TIL	Tumor infiltrating lymphocytes
TUNEL	Terminal deoxynucleotidyl transferase dUTP nick end labeling
ZA	Zombie Aqua

Introduction

Cancer is one of the major contemporary global health concerns as it is one of the leading causes of morbidity and mortality worldwide.¹ Consequently, the demand for effective therapeutic solutions is substantial. Conventional approaches for the treatment of cancer include chemotherapy, radiotherapy and surgery. However, despite their effectiveness in many situations, they often come with adverse effects and/or limitations. This highlights the need for novel strategies that improve cancer treatment. In this regard, during the past years, mRNA therapeutics have been showing great potential.²⁻⁴ The use of mRNA as therapeutic has several advantages over for instance, proteins or DNA. For example, mRNA has a better safety profile than DNA or proteins since it does not integrate in the host genome—like DNA does—and induces weaker immune responses when compared to proteins. Nonetheless, the intrinsic physicochemical properties of mRNA (large, polyanionic and hydrophilic) and the high frequency of RNA endonucleases in body fluids and tissues hamper its direct administration.² Therefore, in order to be able to efficiently deliver mRNA and other nucleic acids, a drug delivery system is required. Currently, a diverse array of nanocarriers are under investigation for nucleic acid-delivery. They can be distinguished into two main types: viral and non-viral delivery systems.^{5,6} The viral delivery vectors have shown great clinical success in the treatment of various diseases.⁷ However, limitations such as viral-induced immunogenicity, pay-load size constraints and pre-existing immunity have pushed forward the development of non-viral delivery systems. Of the non-viral mRNA-delivery systems, lipid-based nanocarriers are the most advanced ones.^{8,9} In fact, three lipid nanoparticle (LNP)-encapsulated nucleic acid therapeutics have reached the clinic: Onpattro, an siRNA used to treat polyneuropathies caused by hereditary transthyretin-mediated amyloidosis (hATTR), and BNT162b2 and mRNA-1273, two mRNA vaccines used against the severe acute respiratory syndrome coronavirus 2 (SARS-CoV-2).¹⁰⁻¹³

LNPs generally consist of: 1) an ionizable lipid or lipid-like material, 2) a non-cationic (phospho)lipid (also known as helper lipid), 3) a cholesterol derivate, 4) a PEG-lipid conjugate and 5) a nucleic acid cargo (in our case, mRNA). The vast variety of lipid chemical structures and the possibility to use them in different ratios leads to an almost infinite amount of LNP formulations with different physicochemical characteristics and *in vitro* and *in vivo* transfection efficacies.^{9,14} Moreover, if using a one-variable-at-a-time approach, the number of formulations to test and the number of optimization rounds to perform can be huge and almost impossible to perform in an *in vivo* set up. Additionally, these approaches do not take into account potentially significant second-order interactions between the different parameters. This screening task can be made easier by using Design of Experiments (DoE) methodologies. DoE methodology refers to a structured approach for conducting an experiment to

understand and manipulate multiple independent variables simultaneously, in order to observe their impact on the outcome of interest, in this case transfection efficiency.

Moreover, it is known that there are substantial translatability issues between *in vitro* and *in vivo* models and also between preclinical models and patients. This is attributable to the fact that *in vitro* models lack the biological context, such as the interactions with various cell types and tissues and the influence of the immune system, that is essential for understanding LNP behavior and performance in a clinical setting. Regarding the lack of translatability between animal models and humans, it is due to the fact that there are biological processes that are inherent and exclusive of the human biology and disease. Furthermore, animal testing faces ethical concerns as well as practical limitations in terms of resources and effort. Thus, in order to circumvent the limitations that *in vitro* and *in vivo* models involve, scientists have been developing 3D culture systems with more relevant cell sources than the classical cell lines. Some examples are the popular organoids, the organ-on-a-chip devices or the bioprinting using stem cells or primary cells. For the treatment of certain types of cancer, one of the routes of administration that has been explored for mRNA LNPs is the intratumoral since it allows to avoid the drawbacks related to systemic administration of LNPs, namely the low therapeutic index or the high toxicity. Therefore, in this paper, we sought to develop an *ex vivo* culture model with precision-cut tumor slices. We opted for this 3D model since it has the ability to preserve the cellular and tissue architecture and also allows to maintain the tumor-stroma interaction. Additionally, with this approach, the tumor heterogeneity is conserved; not only it includes the tumor cells but also, the primary tumor-infiltrating lymphocytes, the endothelial cells and the fibroblasts, which are essential to predict the treatment efficacy. Besides that, this platform could be used for personalized therapeutic screenings since it can also be performed with human tumor biopsies in a rapid and reproducible manner.¹⁵⁻¹⁸

In this paper, we developed an *ex vivo* tumor slice platform for screening of LNP libraries upon intratumoral administration. We present an experimental method for preparation of precision-cut tumor slices with a survival of up to 5 days. We show that MC38 tumor slices remain viable during *in vitro* culturing and that both the lymphocyte and endothelial cell populations, a part from the tumor cells, survive at least up to 48 hours. Finally, we show that the tumor slices can be used to screen mRNA LNP libraries.

Materials and Methods

Cell culture

MC38 murine colorectal carcinoma cell line was used for this project. Cells were cultured in DMEM (Thermo Fisher Scientific), supplemented with 10% fetal bovine serum (FBS) (Gibco), 1% penicillin-streptomycin (P/S) antibiotic (Gibco), 1% non-essential amino acids (NEAA) (Sigma) and 1% sodium pyruvate (Sigma). Cell culture was performed according to normal culturing conditions at 37°C in 5% CO₂ conditions in a sterile environment.

Animal tissue

C57BL/6J mice of 7-10 weeks of age were obtained from Charles River Laboratories. Mice were bred and maintained in accordance with animal experimental guidelines of the Instantie voor Dierenwelzijn Utrecht (AWB Utrecht). All mouse experiments were performed accordingly to the approved work protocol (AVD10800202115026). For experimental procedures, MC38 cells were detached and resuspended in plain DMEM at a concentration of 1×10^6 cells/mL. Bilateral subcutaneous inoculation of $4-5 \times 10^5$ cells/flank was performed for MC38 tumor generation. At tumor dimensions of 1000 mm³ the mice were euthanized by cervical dislocation and tumors harvested by surgical excision. Immediately after collection, tumors were immersed in ice-cold DMEM, composition as described above, containing 3% P/S.

Preparation of precision-cut tumor slices

Tumor cores of 8 mm diameter were prepared using a biopsy punch and subsequently embedded in 2% (w/v) low-melting point agarose (Promega). Before slicing, all equipment was sterilized with 70% EtOH. Embedded cores were sliced into 300 µm thick slices using a Leica VT 1000s Vibratome (Leica Biosystems), with the following settings: amplitude 1-2 mm, frequency 90 Hz and speed 0.3-1 mm/s, depending on tissue consistency. Slicing was performed in ice-cold PBS containing 3% P/S. The obtained tumor slices were transferred and stored in DMEM containing 3% P/S until finishing of slicing procedure.

Culture conditions of tumor slices

Obtained tumor slices were washed with PBS + 3% P/S and placed on Millicell Cell Culture Inserts (12 mm, 0.4 µm, PTFE; Merck Millipore®) in 24-well cell culture plates containing 650 µl of DMEM + 3% P/S. Transferring of the slices was performed using a sterile spatula. Tumor slices were incubated at normal culturing conditions. After 24 hours, tissue slices were washed with PBS + 3% P/S and medium was replaced with DMEM + 1% P/S. Medium was changed every consecutive day for the entire length of the experiments.

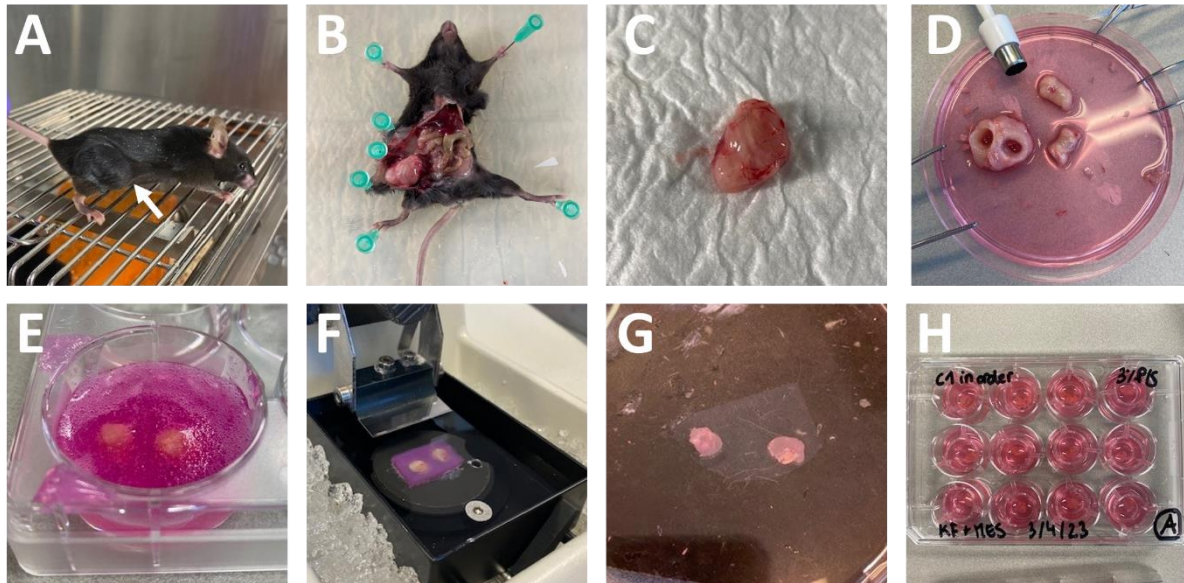


Figure 1 - Graphical illustration of the preparation and culturing of precision-cut tumor slices. (A) C57BL/6 mouse with subcutaneous tumor in the flank region, as indicated by the arrow. (B) Dissected mouse showing the location of tumor origin. (C) Excised tumor with maximum dimensions of 1000 μm^3 . (D) Preparation of 8 mm biopsy punches. (E) 2% w/v low-melting point agarose embedding. (F) Slicing set-up of vibratome. (G) Obtained 300 μm thick tumor slices (still attached to agarose). (H) Slices placed on inserts in a cell culture plate.

Microscopy

Histology

Slices were fixed at various time points during culturing by fixing overnight in 4% PFA. Fixed slices were embedded in paraffin, 5 μm thick sections were prepared and placed on glass microscopy slides. For morphological analysis, the formalin-fixed, paraffin embedded (FFPE) sections were stained with hematoxylin and eosin (H&E) following the standard procedure and analyzed at various magnifications using an Olympus BX43 microscope.

Immunofluorescent stainings

For cell viability assessment, immunofluorescence Ki-67 and TUNEL assays were performed. For Ki-67 staining, FFPE slides were deparaffinized with Tissue-Clear and rehydrated in ethanol (EtOH). Heat-induced antigen retrieval was performed by boiling in citrate buffer (pH=6), before permeabilizing with 0.1% v/v Triton X-100. After blocking in 5% BSA solution, samples were incubated overnight with Rabbit monoclonal anti-Ki67 primary antibody (Recombinant Anti-Ki67 antibody [SP6] (ab16667), Abcam) in 1% BSA (1:200). After washing in 0.1% v/v PBS-T, samples were incubated with Donkey anti-rabbit IgG-Alexa647 (Donkey anti-Rabbit IgG (H+L) Highly Cross-Adsorbed Secondary Antibody, Alexa647 (A-21206), Invitrogen) in 1% BSA (1:1000) for 1 hour. Nuclear counterstain was performed using DAPI in 1% BSA (1:2000) for 15 min. Fixed Ki-67-stained slides were analyzed at wavelength 488 (FITC channel) at various magnifications using a Zeiss Axio Observer Z1 microscope.

The TUNEL assay, using TUNEL Assay Kit - BrdU-Red (ab66110), Abcam), for detecting apoptosis was performed in accordance to the provided manufacturers protocol. For nuclear counterstaining DAPI (1:2000) was used. Fixed TUNEL stained slides were analyzed at wavelength xxx (PE channel) at various magnifications using a Zeiss Axio Observer Z1 microscope.

Viability assay

Cell viability of cultured tumor slices was assessed for 8 consecutive days after slicing, using the CellTiter 96[®] Aqueous One Solution Cell Proliferation Assay (Promega). Slices were cultured according to methods described above. For the MTS assay, slices were washed in PBS before transferring to a 48-wells plate containing 480 µl of fresh DMEM + 1% P/S + MTS reagent (6x diluted) and incubating for 2 hours. Medium was transferred to a 96-well plate, absorbance was read at 490 nm and normalized to blanks. After the MTS assay, slices were washed in PBS before returning them to inserts in fresh culture medium and continued standard culture until consecutive MTS assay.

Identification of cell populations by flow cytometry

For investigating the cell populations present in cultured tumor slices, slices were prepared as described previously. Directly after slicing, 24 hours and 48 hours of culturing, single cell suspensions were prepared of the tumor slices. Briefly, approximately 8 slices were pooled, weighed and subsequently dissociated mechanically using a surgical blade. After addition of enzymatic digestion buffer (1 µg/mL DNase I + 2,75 mg/mL Collagenase type 3 in DMEM), samples were incubated shaking at 37°C for 40-60 minutes to ensure proper dissociation. Obtained suspension was resuspended properly, strained through 100 µm cell strainer, and subsequently centrifuged for 7 min at 500g at 4°C. Supernatant was removed and the pellet was resuspended in ACK lysing buffer for 4 minutes before inactivation by addition of PBS and straining through a 70 µm cell strainer. Cells were pelleted as described above and resuspended in plain DMEM twice before counting. 100.000 live cells were seeded per well in a U-bottom 96-wells plate for further antibody staining steps. Plate was centrifuged for 5 min at 500g at 4°C and supernatant was removed. Cells were resuspended in 50 µl of Zombie Aqua (ZA) and TruStain (2 µg/mL) in PBS and subsequently incubated for 15-20 minutes on a plate shaker. Plate was centrifuged as mentioned before and supernatant removed before resuspension of the pellet in 50 µl of corresponding antibody solutions. After 20-30 minutes of incubation, cells were washed twice with 2% PBSA and subsequently resuspended in 200 µl 2% PBSA for analysis by FACS, using a BD LSRFortessa flow cytometer (BD Biosciences). Antibodies used for staining were CD45-BV711 (BD Biosciences) and CD31-FITC (Thermofisher).

LNP preparation and characterization

Lipids

S-Ac7-Dog was used as the ionizable lipid for electrostatic lipid:mRNA complexation. Lipid was kindly gifted by Ethernal Immunotherapies Nv. and dissolved in ethanol to a concentration of 38.37 mg/mL. Additional used (phospho)lipids for LNP formulation were DSPC, cholesterol and DMG-PEG2000. (see Table 1) Solid lipids were dissolved in ethanol and stock solutions were stored at -20 °C.

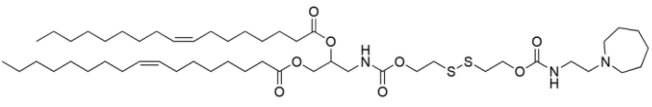
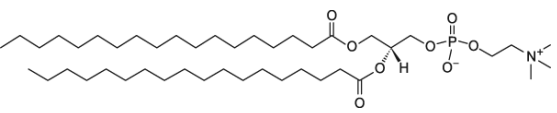
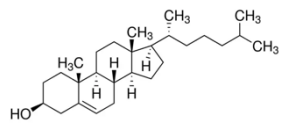
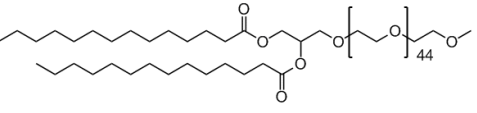
Lipid	Structure	Molecular weight (Da)
S-Ac7-Dog		968,5
DSPC		790,15
Cholesterol		386,65
DMG-PEG2000		2509,2

Table 1 – Lipids used for LNP formulation. S-Ac7-Dog – DSPC – 1,2-distearoyl-sn-glycero-3-phosphocholine (18:0 PC); Cholesterol – (Chol); DMG-PEG2000 – 1,2-dimyristoyl-rac-glycero-3-methoxypolyethylene glycol-2000.

Formulation of LNPs

LNPs were synthesized by mixing an aqueous phase containing Fluc mRNA (Ethernal Immunotherapies Nv.) with an ethanol phase containing the lipids in a NanoAssemblr Benchtop™ microfluidic cartridge (Precision Nanosystems). In short, the aqueous phase was prepared in a 100 mM sodium acetate buffer (pH 4) with Fluc mRNA (Ethernal Immunotherapies Nv.) The ethanol phase was prepared by mixing s-Ac7-Dog, DSPC, cholesterol, and DMG-PEG2000 in varying predetermined ratios. Syringe pump (NanoAssemblr® Benchtop™) was used to mix ethanol and aqueous phase at a 3:1 ratio in the microfluidic chip. Obtained LNPs were dialyzed overnight against a 1000 fold excess of TBS (20 mM Tris + 0.9% w/v NaCl, pH 7.4) in a 20K MWCO cassette (ThermoFisher). Concentration and capsulation efficiency were determined using a Ribogreen assay (Quant-iT™ RiboGreen® RNA Assay kit, ThermoFisher). LNP samples were diluted to a concentration of 100 µg/mL using TBS and sucrose (8% w/v) was added as a cryoprotectant before storage at -80°C.

Characterization of LNPs

Size and polydispersity index (PDI) of the LNPs were measured with dynamic light scattering (DLS) in 1x PBS (Sigma), using a Zetasizer Nano ZS (Malvern). Zeta potentials were measured in 10 mM HEPES buffer (pH = 7.4), using a Zetasizer Nano Z (Malvern). The average of three measurements was used to determine the size, PDI and zeta potential of each formulation. For encapsulation efficiency, a Quanti-iT™ RiboGreen® RNA Assay was performed.

In vitro transfections in MC38 cells

Firefly luciferase (Fluc) expression was used to assess transfection efficiency of LNPs in the MC38 cell line. For transfection experiments, MC38 cells from a 80% confluent flask were seeded in a 96-wells plate at a density of 5000 and 10000 cells/well, in 100 µl of DMEM + 1% P/S, containing non-heat inactivated FBS (non-HI DMEM). 24 hours after seeding, LNP formulations were diluted in Opti-MEM to contain 200 ng mRNA in 10 µl of medium. Before addition of LNPs, cells were washed 1x with PBS and medium replaced with Opti-MEM. Subsequently, 10 µl of the diluted LNP samples was added to the medium and resuspended. Lipofectamine 2000 (ThermoFisher) was used as a positive control for transfection. For preparation of lipofectamine samples, 200 ng Fluc mRNA was mixed with 0,5 µl Lipofectamine2000 and 25 µl Opti-MEM and subsequently added to the cells. Cells were transfected for 4 and 24 hours, incubated under normal culturing conditions. After transfection period, medium was removed and cells were washed with PBS. Cell lysates were prepared by addition of 30 µl cell culture lysis reagent and subsequent proper suspension. Luciferase activity was assessed by transferring lysate to a white flat-bottom luminescence 96-wells plate and the subsequent addition of luciferase reagent in a ratio 1:5. After a 2 pause, integrate bioluminescence was recorded over 10 seconds using a Spectramax iD3 (VWR) and subsequently normalized against background.

Transfection of *ex vivo* slices

For transfection of *ex vivo* tumor slices, slices were prepared as described previously. After culturing in 3% P/S overnight, slices were washed in PBS and placed in a 24 wells plate containing 600 µl of Non-HI DMEM + 1% P/S. LNPs were diluted in OptiMEM to a concentration of 0.5 µg mRNA per 50 µl and subsequently added to the medium. Assignment of LNPs to slices was randomized to ensure unbiased distribution of formulations to obtained slices. After 4 hour incubation slices were washed in PBS and transferred to a 48-wells plate containing 200 µl of luciferin reagent. Slices were incubated for 5 min, washed in PBS and transferred to a paper for subsequent Bioluminescence Imaging (BLI). Directly after BLI measurement, slices were snap frozen and stored at -80°C until further processing. Obtained BLI data were quantified and analyzed using M3 vision systems.

Tissue lysates were prepared by transferring tissue slices to homogenization tubes containing 1.4 mm ceramic beads and the subsequent addition of 1x Cell Culture Lysis Reagent (CCLR) (10 µl/mg tissue). Homogenization was performed for 30 seconds at 5000 rpm and samples were left to incubate for 30 minutes. Subsequently, samples were centrifuged for 5 minutes at 10000g at 4°C, the lysate supernatant transferred to clean Eppendorf and stored at -80°C until further processing. For analysis, lysate was transferred to a white opaque 96-wells plate and bioluminescence was measured by a luciferase assay similarly as described above, using a Spectramax iD3 (VWR).

Results

Developing an *ex vivo* tumor slice platform for LNP library screening

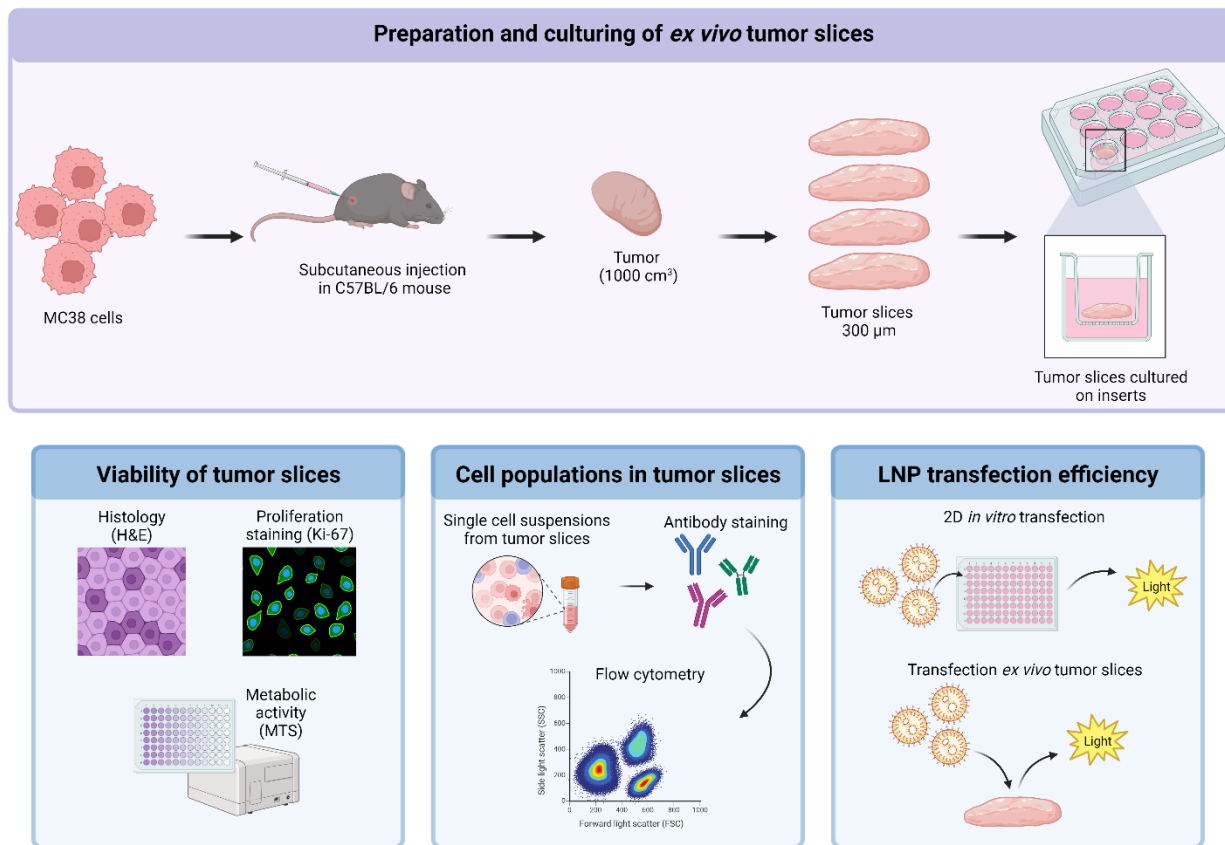


Figure 2 – Graphical schematic of the development of an *ex vivo* tissue slice platform for LNP library screening. Key steps include the preparation and culturing of the tumor slices and the validation of the tissue slice platform. For this, the viability of the slices was assessed using various assays. Subsequently, the perseverance of (primary) cell populations within the slices was investigated by flowcytometry. Lastly, the transfection efficiency of a Fluc mRNA-LNP library was evaluated both *in vitro* and on the tumor slices.

The effect of culturing on *ex vivo* tumor slice viability

Firstly, we aimed to examine the effect of culturing on the viability of the *ex vivo* tumor slices. As a quantitative analysis of viability, we used a colorimetric MTS assay to measure the metabolic activity of the slices over time. The preparation of the tumor slices was designed to generate standardized 300 µm thick slices with an approximate diameter of 8 mm. As all slices were also treated similarly, we considered a drop in metabolic activity as a drop in viability. As shown in *Figure 3-A*, the viability of the slices remained relatively constant, especially for the first 48 hours. A general decline in viability was observed when culturing over a longer period of time. Furthermore, a noticeable reduction in viability was observed when the culture medium was not refreshed over the weekend. Of note, tumor slices were also treated with Triton-X, a commercially available detergent known to cause cellular or tissue

damage at high concentrations, in order to demonstrate a decrease in cellular viability (*Figure 3-A*) as a control of the assay.

Alongside the results observed in the MTS assay, the tissue morphology and proliferative capacity of the slices were investigated by means of microscopy. The morphology changes in the tumor tissue upon slicing and culturing were assessed using an H&E staining (*Figure 3-B*) and the proliferative capacity, with an immunofluorescent staining of Ki-67, a nuclear proliferation marker (*Figure 3-C*).^{19,20} In order to assess the slicing effect on both the morphology and viability, an unsliced tumor was used as control. As seen in *Figure 3-B*, tumor tissue generally displays a chaotic and disorganized arrangement. Different growth patterns can be observed due to cell growth in various orientations and directions. Although, metabolic activity does not drop notably over the first 48 hours of culturing, morphological changes in cultured tumor tissue can be discerned within this time frame. Increased nuclear and cytoplasmic condensation are observed in tumor slices cultured for 48 hours.

A similar trend is observed in the cellular proliferative activity of cultured slices. Ki-67 expression substantially decreases in tumor slices the longer they are cultured (*Figure 3-C*). Nuclear condensation and the rounding of the nuclei can be observed when looking at the DAPI stained nuclei, in a similar trend seen in the H&E staining. Of note, tumor slices treated with TX-100 overnight, show an evident drop in Ki-67 expression, in order to demonstrate a similar decrease in cellular viability as used in the MTS assay. For validation purposes, alongside the Ki-67 staining, a TUNEL assay was performed to assess apoptosis levels over time (*Figure S-1*). While a trend of increase in fluorescent signal over time could be suggested, no hard conclusions were drawn from this assay, due to uncertainties of the assay's reliability.

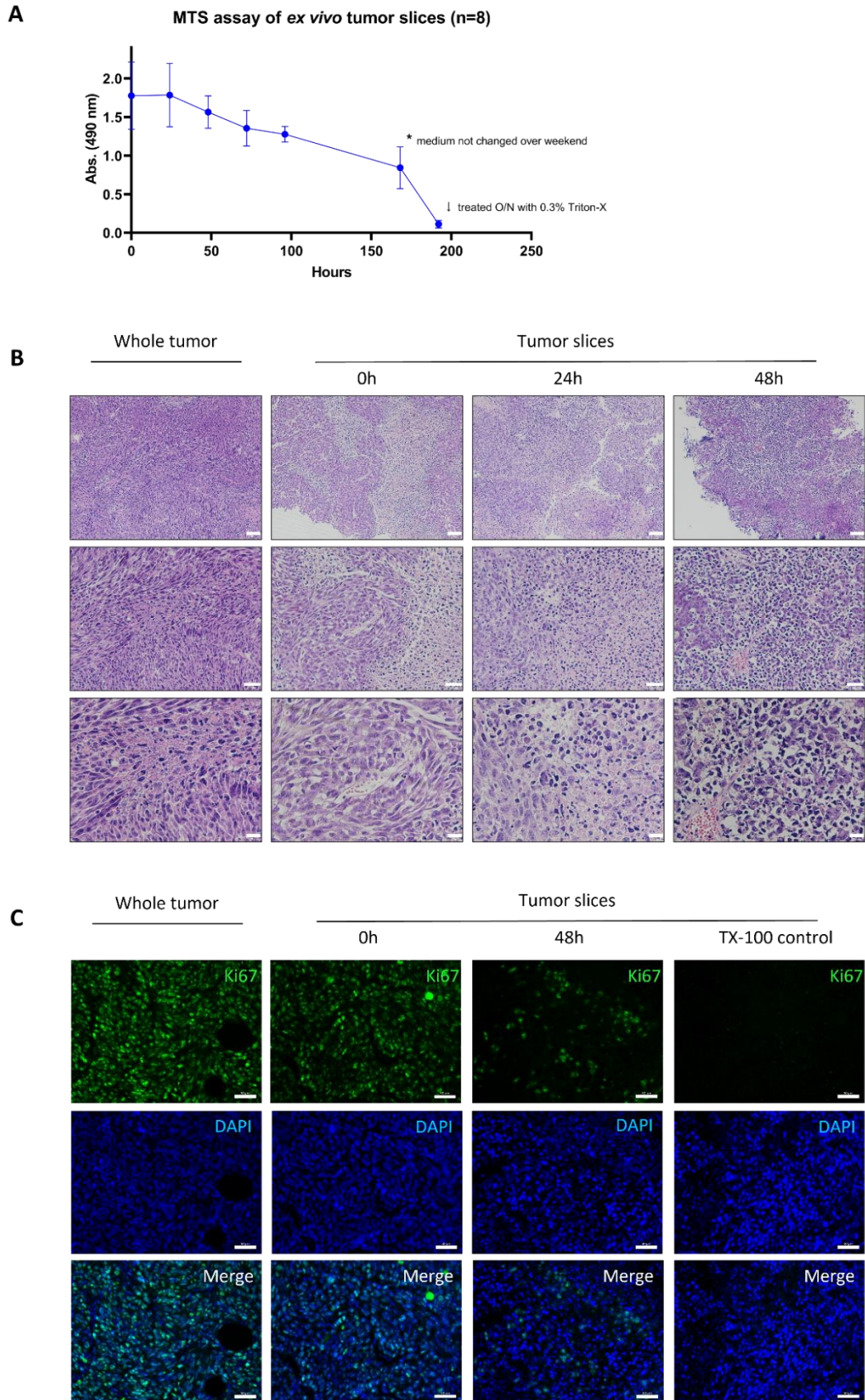


Figure 3 - Viability of *ex vivo* tumor slices. (A) Assessment of viability and metabolic activity of slices over time by MTS assay. (B) Histological analysis of morphology changes in tumor slices over time by H&E staining. Rows indicate increasing magnifications. Scale bars represent 100, 50, and 20 μm from top to bottom. (C) Immunofluorescent assessment of cell proliferation in tumor slices by Ki-67 expression over time. Scale bars represent 50 μm .

Quantification of cell populations present in cultured tumor slices

We conducted an in-depth examination of the cell populations present in *ex vivo* tumor slices over a cultivation period of 48 hours. We aimed to investigate the effect of culturing on both the cell viability, as well as the presence of specific cellular subpopulations, such as tumor infiltrating lymphocytes (TIL) and endothelial cells. Single cell suspensions were successfully prepared from *ex vivo* tumor slices after 0, 24 and 48 hours after culturing, using mechanical dissociation and subsequent enzymatic digestion. We found that distinct cell populations within the tumor microenvironment could successfully be detected and distinguished by immunolabeling and subsequent flow cytometric analysis. CD45+ cell population was identified as TILs, CD45-/CD31+ cells were classified as endothelial cells, and the remaining cells were assumed to be tumor cells.

It was found that the cell viability remained relatively stable during the cultivation period. (Figure 4-A) A slight decline in cell viability is observed over time, as the average percentage drops from approximately 50% at 0 hours to 36% after 48 hours. Nevertheless, these flow cytometric results seem to match the same trend as observed in the MTS assay. Noteworthy is the difference in cell viability between the unsliced tumor sample and the *ex vivo* tumor slices taken directly after slicing. (Figure 4-A) This observed variation highlights the inherent heterogeneity of tumors, where cell viability of tumor tissue varies greatly based on the specific region sampled. Previous experiments have indicated that the cell viability after slicing (0 hours) can also closely resemble tumor viability before slicing (Figure S-2). In this case, the viability of the unsliced tumor was 83.4% and the viability directly after slicing 81.6%.

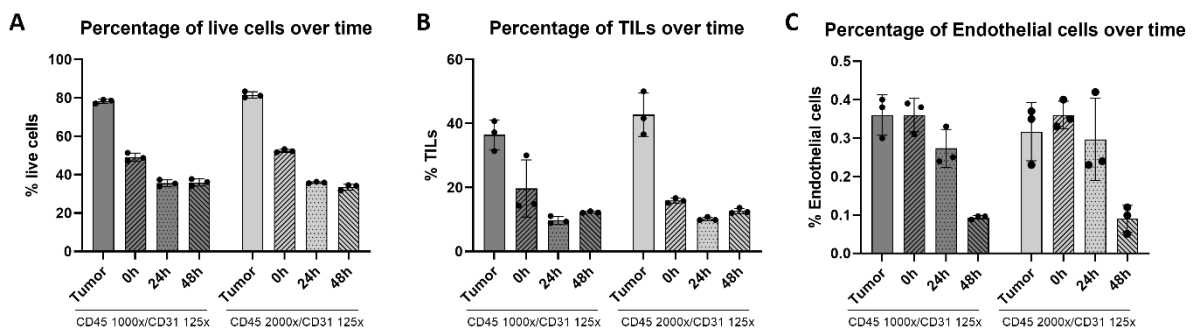


Figure 4 – Flow cytometric analysis of the effect of culturing on cell viability and presence of cell populations in *ex vivo* tumor slices. (A) Quantification live cells (ZA-) as a percentage of total cells. (B) Quantification of TIL population (CD41+/CD31+) as a percentage of total live cells. (C) Quantification of endothelial cell population (CD31+/CD41-) as a percentage of total live cells. Error bars represent standard deviations from three technical replicates.

Additionally, in the cultured tumor slices, distinct cell populations for the tumor microenvironment, including TILs and endothelial cells, were discerned and quantified over the cultivation period. The analysis provides a deeper understanding of the changes in cell population numbers over time, as well as providing some insight in the effect of chosen culture set-up, such as medium composition, on

survival of different cellular subgroups. *Figure 4-B* and *4-C* illustrate the presence of TILs and Endothelial cells even after 48 hours of culturing, respectively. However, a considerable drop—approximately 74% decline, from an initial value of 0.36% at 0h to a final value of 0.094%—is observed in endothelial cells for the 48 hours samples, indicating a substantial loss of this particular population.

Design & characterization of LNP libraries

We strategically designed the Fluc-mRNA LNP library using a Design of Experiment (DoE) methodology. This approach was employed to limit the amount of LNP formulations needed to explore the effects of multiple variables on transfection efficiency at the same time. The rationale behind this DoE approach was to create a LNP library with a diverse array of potential formulations, allowing us to gain valuable insights into the effect of lipid ratios on mRNA delivery efficacy. Next to this, a validation library was generated, based on priorly acquired *in vivo* data. This validation library comprised of both well-performing and poorly-performing LNPs in an *in vivo* setting. The inclusion of these validation formulations aimed to validate and compare the obtained findings for the DoE library. Our formulations consists of different ratios of ionizable lipid (s-Ac7-Dog), phospholipid (DSPC), helper lipid (cholesterol) and PEG-lipid (DMG-PEG2000), complexed with Fluc mRNA in a 10:1 molar ratio. The DoE library and validation library, along with their formulation specifics, are presented in *Figure 5-B*. The LNPs were synthesized using a microfluidic mixing approach, as elaborately described priorly, to ensure uniformity and precision of LNP formulations. To investigate the influence of lipid composition on LNP formation, the generated LNPs were subsequently subjected to comprehensive characterization. Dynamic Light Scattering (DLS) analysis showed an average particle size between 60 and 120 nm, with polydispersity indexes (PDIs) <0.2, indicating particle sizes within appropriate range and uniform, well-dispersed particle size distribution (*Figure 5-C*). Zeta potential measurements indicated a surface charge between -7 and 1 mV (*Figure 5-D*). Encapsulation efficiencies were evaluated using a Ribogreen assay, and showed high encapsulation efficiencies above 83% (*Figure 5-E*). As the LNPs are stored at -80°C for further experiments, the (size) stability of LNP formulations was evaluated before and after freezing using DLS (*Figure 5-F*). All formulations, with the exception of LNP10, demonstrated adequate stability after thawing. Of note, LNP10 is the only formulation containing <1% PEG, a condition known to cause aggregation. Characterization of the validation library was performed similarly and shown in *Figure S-3*.

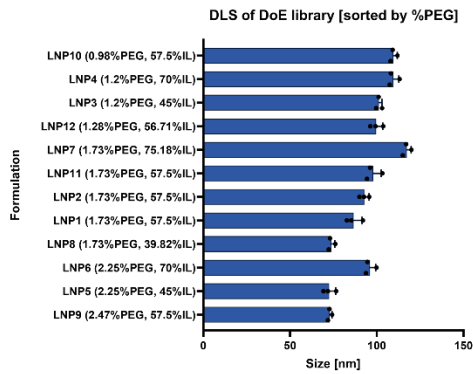
A



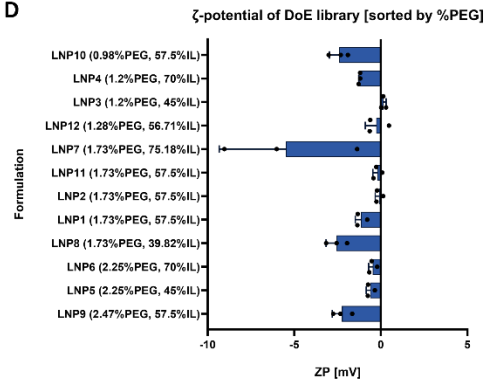
B

	LNP #	Ioniz. lipid	Helper lipid	Lipid 3	Lipid 4	Ioniz. Lip : mRNA (molar ratio)	Lipid ratios
DoE Library	1	S-Ac7-DOg	DSPC	Cholesterol	DMG-PEG2000	10	57.5 / 17.07 / 23.7 / 1.73
	2	S-Ac7-DOg	DSPC	Cholesterol	DMG-PEG2000	10	57.5 / 2.93 / 37.84 / 1.73
	3	S-Ac7-DOg	DSPC	Cholesterol	DMG-PEG2000	10	45 / 13.54 / 40.26 / 1.2
	4	S-Ac7-DOg	DSPC	Cholesterol	DMG-PEG2000	10	70 / 13.54 / 15.26 / 1.2
	5	S-Ac7-DOg	DSPC	Cholesterol	DMG-PEG2000	10	45 / 13.54 / 39.21 / 2.25
	6	S-Ac7-DOg	DSPC	Cholesterol	DMG-PEG2000	10	70 / 13.54 / 14.21 / 2.25
	7	S-Ac7-DOg	DSPC	Cholesterol	DMG-PEG2000	10	75.18 / 6.46 / 16.63 / 1.73
	8	S-Ac7-DOg	DSPC	Cholesterol	DMG-PEG2000	10	39.82 / 6.46 / 51.99 / 1.73
	9	S-Ac7-DOg	DSPC	Cholesterol	DMG-PEG2000	10	57.5 / 6.46 / 33.57 / 2.47
	10	S-Ac7-DOg	DSPC	Cholesterol	DMG-PEG2000	10	57.5 / 6.46 / 35.06 / 0.98
	11	S-Ac7-DOg	DSPC	Cholesterol	DMG-PEG2000	10	57.5 / 10 / 30.77 / 1.73
	12	S-Ac7-DOg	DSPC	Cholesterol	DMG-PEG2000	10	56.71 / 14.43 / 27.58 / 1.28
Validation Library	13	S-Ac7-DOg	DSPC	Cholesterol	DMG-PEG2000	10	64.21 / 14.63 / 20.13 / 1.03
	14	S-Ac7-DOg	DSPC	Cholesterol	DMG-PEG2000	10	61.34 / 17.5 / 20.13 / 1.03
	15	S-Ac7-DOg	DSPC	Cholesterol	DMG-PEG2000	10	50 / 10 / 38.5 / 1.5
	16	S-Ac7-DOg	DSPC	Cholesterol	DMG-PEG2000	10	64.26 / 12.28 / 20.96 / 2.5
	17	S-Ac7-DOg	DSPC	Cholesterol	DMG-PEG2000	10	64.26 / 7.5 / 27.06 / 1.18
	18	S-Ac7-DOg	DSPC	Cholesterol	DMG-PEG2000	10	40.41 / 16.65 / 41.76 / 1.18
	19	S-Ac7-DOg	DSPC	Cholesterol	DMG-PEG2000	10	44.06 / 7.5 / 45.94 / 2.5

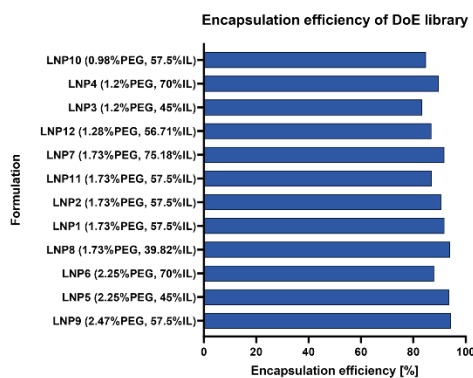
C



D



E



F

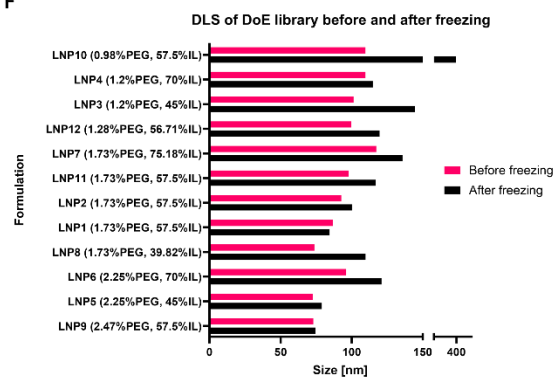


Figure 5 - Characterization of DoE LNP library. (A) Schematic overview of LNP formulation. (B) Formulation characteristics of DoE and validation library. (C) Size of DoE LNP formulations, measured by dynamic light scattering. Values represent the mean of three technical measurements. (D) Zetapotential of DoE LNPs, measured by laser Doppler electrophoresis. Values represent the mean of three technical measurements. (E) mRNA encapsulation efficiency of DoE LNP formulations, measured by Ribogreen assay. Values represent the mean of duplicate technical measurements. (F) Size of DoE LNP formulations before and after freezing, measured by dynamic light scattering. Values represent the mean of three technical measurements, in two independent experiments.

2D *in vitro* transfection efficiency of DoE library in MC38 cells

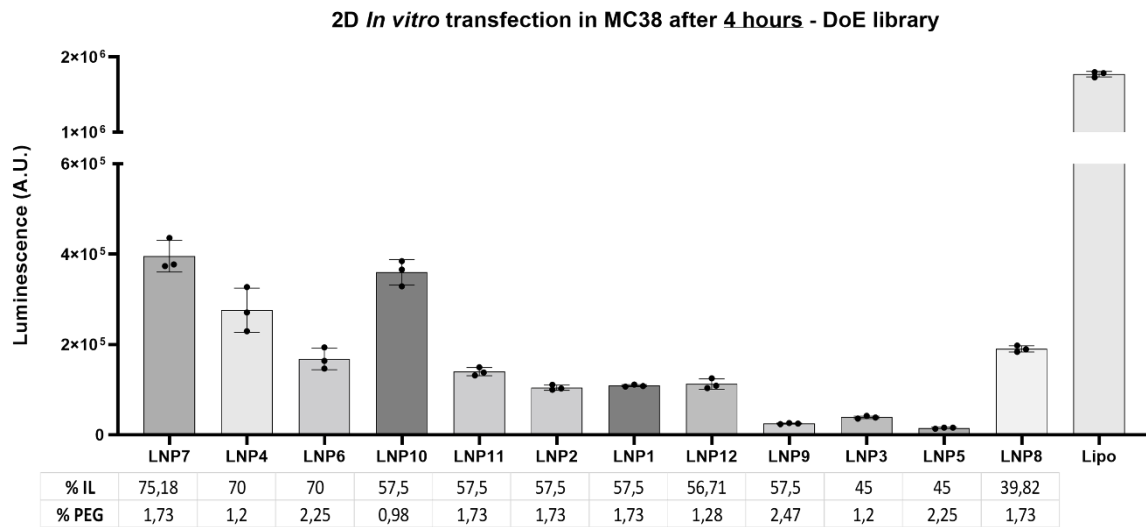


Figure 6 - 2D *in vitro* transfection of DoE library in MC38 cells measured by luciferase assay after 4 hours. Cells were transfected with LNPs or lipofectamine, equivalent to 200 ng Fluc mRNA per well (10000 cells). Luciferase activity was measured after 4 hours by addition of luciferase reagent to cell lysates, and expressed in luminescence (A.U.). Indicated data points (n=3) represent the mean of duplicate measurements of biological replicates within the same experiment and normalized for background signal.

Transfection efficiency of the different LNP formulations was investigated by measuring luciferase activity in MC38 tumor cells, a murine model for colorectal carcinoma (*Figure 6*). Luciferase activity, measured in generated (bio)luminescence upon addition of luciferase reagent to the lysates of transfected cells, served as a quantitative indicator of successful delivery and expression of Fluc mRNA by LNPs. It was found that the percentage of ionizable lipid (%IL) seemed to be the most important factor for transfection efficiency. Formulations with higher %IL, seemed to perform better than formulations with lower %IL. Next to this, it seemed that the percentage of PEG lipid (%PEG) is the second factor affecting transfection. Formulations with similar %IL, but higher %PEG perform worse than formulations with lower %PEG. Of note, LNP8 is the only formulation that does not follow this trend, as relatively high transfection efficiencies are observed, despite of its relatively low %IL & a high %PEG. 2D *in vitro* transfection efficiency of the validation library is shown in *Figure S-4*.

Transfection of *ex vivo* tumor slices

The primary objective of our study was to assess the transfection efficiency of the LNP library using the tumor slice platform. Slices were prepared and cultured according to established methods and subsequent transfections were conducted over a 4-hour period. For quantification of luciferase activity in the transfected slices, BLI (*Figure 7*) and analysis of tissue lysates (*Figure 8*) were used. BLI facilitated the real-time visualization of luciferase expression and the tissue lysates were used to ensure comprehensive understanding of the transfection outcomes. Comparison of the results of the two read-outs confirmed that the transfection and subsequent detection of luciferase activity was successful. Transfection using the validation library was also conducted, the outcomes are illustrated in *Figure S-5* and *Figure S-6*.

Our findings demonstrate that inter-formulation differences in transfection efficiency can be detected by using tumor slices, something that we previously only could observe in an *in vitro* set-up. Mirroring the *in vitro* context, the %IL seems to be the driving factor for transfection, with higher %IL correlating positively with enhanced transfection efficiency across various formulations. The effect of %PEG on transfection efficiency seems to be less pronounced in the *ex vivo* setting. Formulations with comparable %IL but higher %PEG do not exhibit the speculated reduction in transfection.

Notably, LNP10 and lipofectamine demonstrate a significant decrease in transfection efficiency in the *ex vivo* model, compared to the *in vitro* counterpart. Furthermore, a continued deviation is observed for LNP8 from the anticipated %IL-driven trend, persisting both in the *in vitro* and *ex vivo* settings.

Ex vivo transfection of tumor slices - DOE library

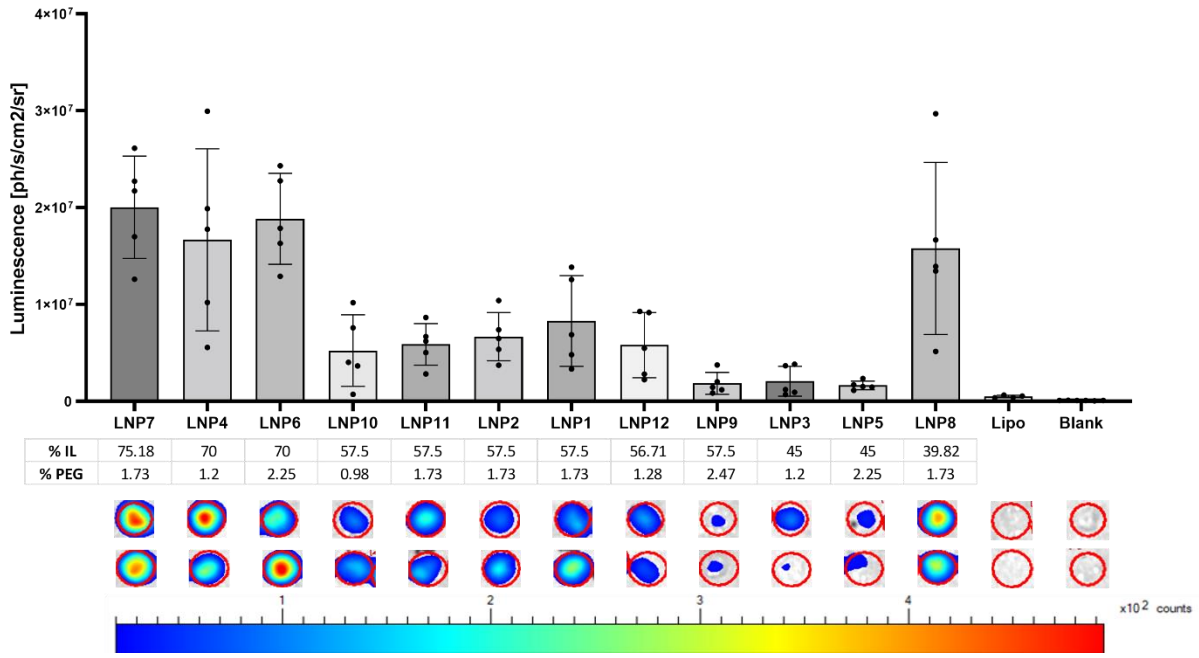


Figure 7 – Transfection of ex vivo tumor slices with DoE library measured by BLI after 4 hours. Slices were transfected with LNPs or lipofectamine, equivalent to 0.5 µg Fluc mRNA per slice. Transfection efficiency was measured after 4 hours by BLI, after 5 min incubation of the slice in luciferin. The emitted bioluminescence is representative of luciferase activity in transfected slices, expressed in photons emitted per second from the specified area in all directions (ph/s/cm²/sr). Indicated data points represent biological replicates (n=5) measured in two independent experiments with tumors originating from two distinct mice.

Tissue Lysates transfection of ex vivo tumor slices - DOE library

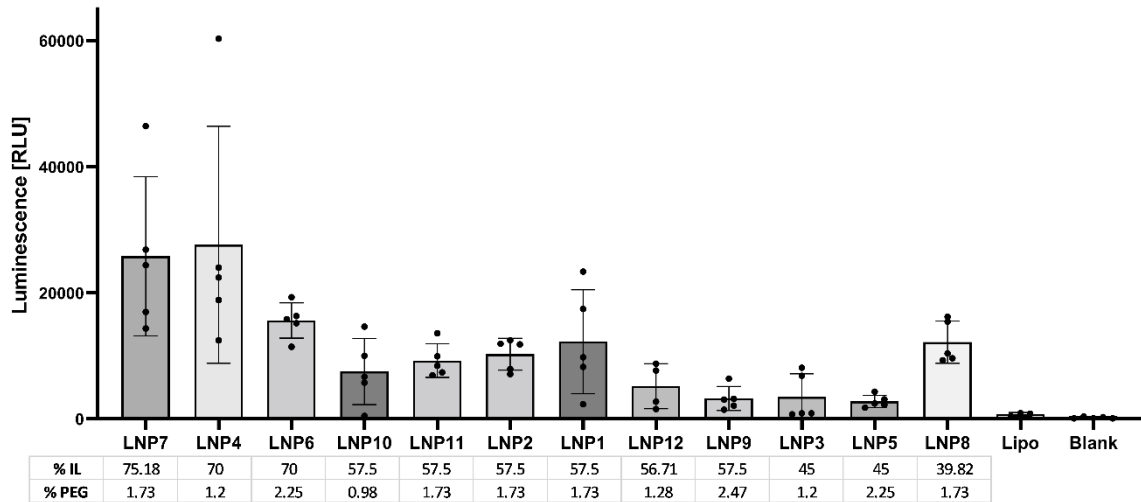


Figure 8 – Transfection of ex vivo tumor slices with DoE library measured by tissue lysates after 4 hours. Luciferase activity was determined for the tissue lysates obtained from snap-frozen transfected slices, the same samples used for BLI measurements. Luciferase activity was quantified by measuring luminescence emitted upon addition of luciferase reagent and expressed in relative light units (RLU). Indicated data points represent the mean of duplicate measurements for the same biological replicates (n=5) used for BLI.

Discussion

In this report we describe the preparation and cultivation of precision-cut tumor slices (PCTS) from MC38 tumors, grown subcutaneously in C57BL/6 mice, as a novel platform to perform screenings of LNP libraries. For the development of mRNA-based therapies for cancer, the intratumoral route of administration is currently being explored to avoid the drawbacks of systemic delivery. We sought a relevant 3D model to potentially mimic this clinical set-up in order to efficiently screen our LNP library. The use of PCTS allows us to address some of the limitations associated with conventional 2D *in vitro* and mouse models. For instance, 2D *in vitro* models do not recapitulate the different cell types present in the native tumor environment. Moreover, they do not incorporate the essential extracellular matrix and lack the intricate three-dimensional structure inherent to living tissues. The use of a PCTS-based model allows us to retain the heterogeneity and structural integrity of the tumor environment, thus preserving important biological aspects of the tumor microenvironment. The presence of primary cells in the tumor slices such as TILs, fibroblast, endothelial cells are of utmost relevance to better understand the interaction between different LNP formulations with native cells present in the tumor niche, which are essential for assessing treatment efficacy. PCTS therefore offer a potential platform to investigate mRNA delivery in a biologically more relevant microenvironment compared to traditional *in vitro* systems.

Furthermore, the use of PCTS offers several advantages compared to using mouse models to assess LNP-mediated mRNA delivery. We have noticed that intratumoral administration can be relatively complex and the obtained data has been quite variable (data not yet published). The measured outcome is inevitably influenced by the site of injection in the tumor. Given the tumor's heterogeneity, it is challenging to ascertain whether the injection occurs in a highly viable region or necrotic tissue. Consequently, this will affect distribution and cellular uptake of LNPs, thereby also confounding the measured therapeutic performance of LNPs *in vivo*. The inherent variability between tumors also affects the measured performance. By using a tissue-slice based platform, this variability can be reduced as the entire screening, with multiple replicates, can be performed on the same tumor. In addition, it therefore also enables the reduction of the animals required to test multiple LNP formulations. Altogether, this approach ensures the evaluation of different formulations in a more controlled and reproducible manner, while simultaneously reducing animal usage and associated costs.

The culturing of precision-cut tissue slices has already been used for diverse applications, spanning from toxicological or drug efficacy assessments to pathophysiological studies. This technique has been applied across a wide array of tissue origins, including liver, heart, lung and kidney, highlighting the versatility in terms of research application.^{15,16,21-25} Extensive research has been

conducted to demonstrate that the viability of tissue slices can be maintained for an extended period of time.^{21,23,24} Our primary objective was to determine whether PCTS could potentially serve as a platform for evaluating mRNA delivery by LNPs. To the best of our knowledge, this approach has not yet been explored before, thus serving mainly as a proof-of-concept. While acknowledging the possibilities for protocol enhancements, the primary aim of our viability studies was to see how our current protocol would affect the viability of the tumor slices during a longer cultivation time, without placing excessive emphasis on protocol refinement. Similar as described in literature, we opted to culture on inserts for oxygenation purposes, to ensure tissue vitality.²⁶ Next to this, we have observed that for our experimental set-up a daily change of culture medium is imperative to maintain adequate nutrient supply for our highly metabolically-active slices. This is substantiated by the results of the MTS assay, wherein a clear decline in viability was observed when the medium was not refreshed over the weekend. Nonetheless, the experimental procedures can still be optimized to achieve superior viability and higher cell proliferation rates. Recommendations for optimization could include refining the medium composition to provide cell population-specific nutrients, adjusting the quantity of medium used per slice to account for high metabolism, and fine-tuning the slicing procedure to decrease the tissue damage. In particular, re-evaluating the medium composition and culturing set-up would be of significant value, as it has been shown that using tumor grade-matched matrix support and autologous serum significantly increases tissue morphology, tissue integrity, proliferation and cell viability.¹⁷

Existing literature extensively describes and explores the potential of cultured *ex vivo* tissue slices for therapeutic applications. Commonly, the emphasis is primarily placed on evaluating the maintenance of tissue viability and tissue integrity during the culture period, by looking at the proliferative characteristics (by Ki-67 staining) or histological changes (by H&E staining) of the tissue over the duration of time.^{18–20,23,25,27} However, especially in the field of tumor research, where the heterogeneity of the microenvironment plays such a pivotal role, it is imperative to demonstrate the persistence of various cell types when culturing tumor slices *ex vivo*. Nonetheless, the majority of the studies using PCTS do not explicitly demonstrate this experimentally. In addition to looking at the Ki-67 expression and morphology, we have therefore also investigated the viability and quantified the main groups of cells found in the slices by flow cytometry. This gives us a deeper understanding of the effect that our slicing and culturing protocols have on slice viability, as well as the survival of important populations of primary cells. In this report, we show that we can successfully prepare single-cell suspensions from tissue slices, an approach that, to the best of our knowledge, has not been reported in literature yet. On top of that, we demonstrate a correlation between the MTS viability data and the viability measured by flow cytometry, affirming the reliability of this method. This single-cell suspension approach to studying tissue slices also shows promising potential for studying the transfection of different cell populations within the slice by flow cytometry.

In this study, we demonstrated successful transfection of MC38 tumor slices with LNPs containing Fluc mRNA. We employed two distinct read-out methods, namely bioluminescence imaging (BLI) and analysis of tissue lysates, to quantify transfection efficiency of the LNPs. The consistency between both read-outs provides us a high level of confidence that our transfection was successful and validate the reliability of our measurements.

In essence, when looking at the transfection, this *ex vivo* tumor slice platform can be considered as a system containing biological characteristics native to both *in vitro* and *in vivo* settings. For instance, the enhanced mRNA delivery due to increased percentage of ionizable lipid was similarly observed in both *in vitro* and *ex vivo* systems. Interestingly, lipofectamine, a transfection agent known to efficiently deliver mRNA *in vitro*²⁸, fails to deliver the cargo in the *ex vivo* tissue slices. We hypothesize that this could be due the larger lipo-RNA complexes that are formed, which result in enhanced mRNA delivery compared to the LNPs *in vitro*. Similarly, the aggregating formulation of LNP 10 showed a comparable pattern of increased transfection *in vitro*. The resulting lipofectamine aggregates are known to fail to deliver mRNA *in vivo*, because of the hindered capability to penetrate tissues. When looking at the transfection of PCTS, similar observations of reduced mRNA delivery were seen for lipofectamine, as well as LNP10, underscoring the *in vivo* characteristics of the *ex vivo* tissue slice platform. Interestingly, it was observed that the significance of the %PEG is more pronounced in 2D transfections, compared to the transfection of the *ex vivo* tumor slices. Further comprehensive experiments are needed to elucidate this effect.

Although an *ex vivo* tissue slice platform thus presents as a very interesting approach to assess treatment efficacy in a biologically relevant setting, it remains difficult to establish concordance between *ex vivo* and *in vivo* results. It requires rigorous validation and comparative analyses, as there are many variable factors affecting the outcomes. Furthermore, it is important to note that the method of administering the LNPs in this *ex vivo* setting—namely, adding them to the culture medium—differs significantly from the *in vivo* approach, where LNPs are injected in the tissue directly. Another noteworthy limitation of the platform is that it is considered a laborious and time-consuming effort, due to the careful preparation required for each individual slice.

Hence, PCTS are primarily used in a research setting, as clinical studies demand a high-throughput and routine approach, for which currently more straightforward approaches are available, such as the organ-on-a-chip technology. Nevertheless, PCTS have already found applications in industrial settings.²⁹ With the ongoing advancements in this field, it is probable that tissue slices could soon find more applications in clinical settings. This progress could pave the way for personalized medicine, allowing a deeper understanding of individual patient responses to existing therapies and the development of individually tailored treatments.

Conclusions

In conclusion, we have developed of an *ex vivo* tumor slice platform for screening of LNP libraries. We demonstrate an experimental method for preparation of precision-cut tumor slices with a survival of up to 5 days. We have shown that, using the experimental set up as described, MC38 tumor slices remain viable during *in vitro* culturing up to several days and that different cellular populations—present within normal tumor microenvironment—can be detected up to 48 hours. We have successfully generated and characterized a LNP library for the delivery of Fluc mRNA. Finally, we have demonstrated that the *ex vivo* tumor slice platform can effectively be used to screen LNP libraries for efficacy of mRNA delivery.

This approach offers a versatile platform for screening LNP libraries in a reproducible manner within a biologically relevant context. As advancements are made for this methodology, it allows the efficient screening of therapeutic interventions in a diverse array of tissue types. The adaptability of this approach not only shows high potential for cancer research, but also offers potential for the development of targeted and personalized therapies.

Acknowledgements

I would like to express my heartfelt gratitude to the following persons who have played a significant role in the completion of this research project. Firstly, I am deeply thankful to my supervisor Mariona Estapé Senti for her unwavering guidance and continuous support throughout this entire project. Her passion and enthusiasm have been invaluable to me during this project. Secondly, my thanks go to Dr. Marcel Fens for his expertise, guidance and critical insights. His input has been invaluable in shaping the direction of this research. I extend my thanks to Prof. Raymond Schiffelers for the opportunity to work on this project and within the research group. Special thanks to Arjan Barendrecht for his expert guidance and assistance in microscopy. And finally, I would like to acknowledge my colleagues and peers of the CDL who have provided valuable discussions and support during all stages of this project.

References

1. Siegel RL, Miller KD, Wagle NS, Jemal A. Cancer statistics, 2023. *CA Cancer J Clin.* 2023 Jan;73(1):17–48.
2. Sahin U, Karikó K, Türeci Ö. mRNA-based therapeutics-developing a new class of drugs. Vol. 13, *Nature Reviews Drug Discovery.* Nature Publishing Group; 2014. p. 759–80.
3. Pardi N, Hogan MJ, Porter FW, Weissman D. mRNA vaccines—a new era in vaccinology. Vol. 17, *Nature Reviews Drug Discovery.* Nature Publishing Group; 2018. p. 261–79.
4. Xu S, Yang K, Li R, Zhang L. Mrna vaccine era—mechanisms, drug platform and clinical prospection. Vol. 21, *International Journal of Molecular Sciences.* MDPI AG; 2020. p. 1–35.
5. Tran S, DeGiovanni P, Piel B, Rai P. Cancer nanomedicine: a review of recent success in drug delivery. *Clin Transl Med.* 2017 Dec;6(1).
6. Wicki A, Witzigmann D, Balasubramanian V, Huwyler J. Nanomedicine in cancer therapy: Challenges, opportunities, and clinical applications. Vol. 200, *Journal of Controlled Release.* Elsevier B.V.; 2015. p. 138–57.
7. Paunovska K, Loughrey D, Dahlman JE. Drug delivery systems for RNA therapeutics. Vol. 23, *Nature Reviews Genetics.* Nature Research; 2022. p. 265–80.
8. Pérez-Herrero E, Fernández-Medarde A. Advanced targeted therapies in cancer: Drug nanocarriers, the future of chemotherapy. Vol. 93, *European Journal of Pharmaceutics and Biopharmaceutics.* Elsevier B.V.; 2015. p. 52–79.
9. Hou X, Zaks T, Langer R, Dong Y. Lipid nanoparticles for mRNA delivery. Vol. 6, *Nature Reviews Materials.* Nature Research; 2021. p. 1078–94.
10. Akinc A, Maier MA, Manoharan M, Fitzgerald K, Jayaraman M, Barros S, et al. The Onpattro story and the clinical translation of nanomedicines containing nucleic acid-based drugs. Vol. 14, *Nature Nanotechnology.* Nature Research; 2019. p. 1084–7.
11. Mirtaleb MS, Falak R, Heshmatnia J, Bakhshandeh B, Taheri RA, Soleimanjahi H, et al. An insight overview on COVID-19 mRNA vaccines: Advantageous, pharmacology, mechanism of action, and prospective considerations. Vol. 117, *International Immunopharmacology.* Elsevier B.V.; 2023.
12. Anderson EJ, Roupael NG, Widge AT, Jackson LA, Roberts PC, Makhene M, et al. Safety and Immunogenicity of SARS-CoV-2 mRNA-1273 Vaccine in Older Adults. *New England Journal of Medicine.* 2020 Dec 17;383(25):2427–38.
13. Baden LR, El Sahly HM, Essink B, Kotloff K, Frey S, Novak R, et al. Efficacy and Safety of the mRNA-1273 SARS-CoV-2 Vaccine. *New England Journal of Medicine [Internet].* 2020 Dec 30;384(5):403–16. Available from: <https://doi.org/10.1056/NEJMoa2035389>
14. Zong Y, Lin Y, Wei T, Cheng Q. Lipid Nanoparticle (LNP) Enables mRNA Delivery for Cancer Therapy. *Advanced Materials.* 2023 Nov 17;
15. Sönnichsen R, Hennig L, Blaschke V, Winter K, Körfer J, Hähnel S, et al. Individual Susceptibility Analysis Using Patient-derived Slice Cultures of Colorectal Carcinoma. *Clin Colorectal Cancer.* 2018 Jun 1;17(2):e189–99.
16. Martin SZ, Wagner DC, Hörner N, Horst D, Lang H, Tagscherer KE, et al. Ex vivo tissue slice culture system to measure drug-response rates of hepatic metastatic colorectal cancer. *BMC Cancer.* 2019 Nov 1;19(1).
17. Majumder B, Baraneedharan U, Thiyagarajan S, Radhakrishnan P, Narasimhan H, Dhandapani M, et al. Predicting clinical response to anticancer drugs using an ex vivo platform that captures tumour

- heterogeneity. *Nature Communications* 2015 6:1 [Internet]. 2015 Feb 27 [cited 2023 Nov 6];6(1):1–14. Available from: <https://www.nature.com/articles/ncomms7169>
18. Vaira V, Fedele G, Pyne S, Fasoli E, Zadra G, Bailey D, et al. Preclinical model of organotypic culture for pharmacodynamic profiling of human tumors. *Proc Natl Acad Sci U S A*. 2010 May 4;107(18):8352–6.
 19. Scholzen T, Gerdes J. The Ki-67 protein: From the known and the unknown. Vol. 182, *Journal of Cellular Physiology*. 2000. p. 311–22.
 20. Gerdes J, Lemke H, Baisch H, Wacker H h, Schwab U, Stein H. CELL CYCLE ANALYSIS OF A CELL PROLIFERATION-ASSOCIATED HUMAN NUCLEAR ANTIGEN DEFINED BY THE MONOCLONAL ANTIBODY Ki-67' [Internet]. Vol. 133, *THE JOURNAL OF IMMUNOLOGY*. 1984. Available from: <http://journals.aai.org/jimmunol/article-pdf/133/4/1710/1031649/1710.pdf>
 21. Merz F, Gaunitz F, Dehghani F, Renner C, Meixensberger J, Gutenberg A, et al. Organotypic slice cultures of human glioblastoma reveal different susceptibilities to treatments. *Neuro Oncol*. 2013;15(6):670–81.
 22. Ruigrok MJR, Xian JL, Frijlink HW, Melgert BN, Hinrichs WLJ, Olinga P. siRNA-mediated protein knockdown in precision-cut lung slices. *European Journal of Pharmaceutics and Biopharmaceutics*. 2018 Dec 1;133:339–48.
 23. De Graaf IAM, Olinga P, De Jager MH, Merema MT, De Kanter R, Van De Kerkhof EG, et al. Preparation and incubation of precision-cut liver and intestinal slices for application in drug metabolism and toxicity studies. Vol. 5, *Nature Protocols*. 2010. p. 1540–51.
 24. Gerlach MM, Merz F, Wichmann G, Kubick C, Wittekind C, Lordick F, et al. Slice cultures from head and neck squamous cell carcinoma: A novel test system for drug susceptibility and mechanisms of resistance. *Br J Cancer*. 2014 Jan 21;110(2):479–88.
 25. Jagatia R, Doornebal EJ, Rastovic U, Harris N, Feyide M, Lyons AM, et al. Patient-derived precision cut tissue slices from primary liver cancer as a potential platform for preclinical drug testing. *EBioMedicine*. 2023 Nov 1;97.
 26. Davies EJ, Dong M, Gutekunst M, Närhi K, Van Zoggel HJAA, Blom S, et al. Capturing complex tumour biology in vitro: histological and molecular characterisation of precision cut slices. *Scientific Reports* 2015 5:1 [Internet]. 2015 Dec 9 [cited 2023 Nov 6];5(1):1–17. Available from: <https://www.nature.com/articles/srep17187>
 27. Perocheau D, Gurung S, Touramanidou L, Duff C, Sharma G, Sebire N, et al. Ex vivo primary liver sections recapitulate disease phenotype and therapeutic rescue for liver monogenic diseases. *bioRxiv* [Internet]. 2023 Mar 24 [cited 2023 Nov 6];2023.03.23.533840. Available from: <https://www.biorxiv.org/content/10.1101/2023.03.23.533840v1>
 28. Cardarelli F, Digiacoimo L, Marchini C, Amici A, Salomone F, Fiume G, et al. The intracellular trafficking mechanism of Lipofectamine-based transfection reagents and its implication for gene delivery. *Sci Rep*. 2016 May 11;6.
 29. Hewitt SL, Bailey D, Zielinski J, Apte A, Musenge F, Karp R, et al. Intratumoral IL12 mRNA therapy promotes TH1 transformation of the tumor microenvironment. *Clinical Cancer Research*. 2020 Dec 1;26(23):6284–98.

Supplementary Figures

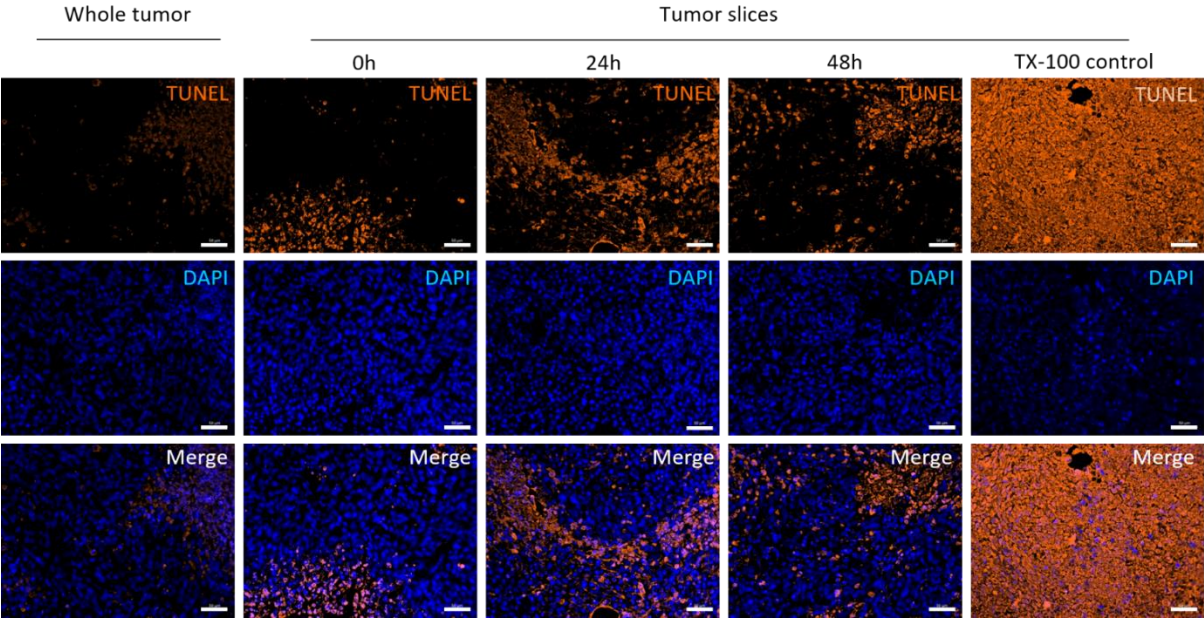


Figure S 1 - TUNEL staining of *ex vivo* tumor slices over time. A TUNEL assay was performed on microscopy sections of the cultured tumor slices. As controls, unsliced tumor (whole tumor) and a slice treated with Triton-X were used. Nuclei were stained with DAPI for localization of the cells. Scale bars represent 50 μ m.

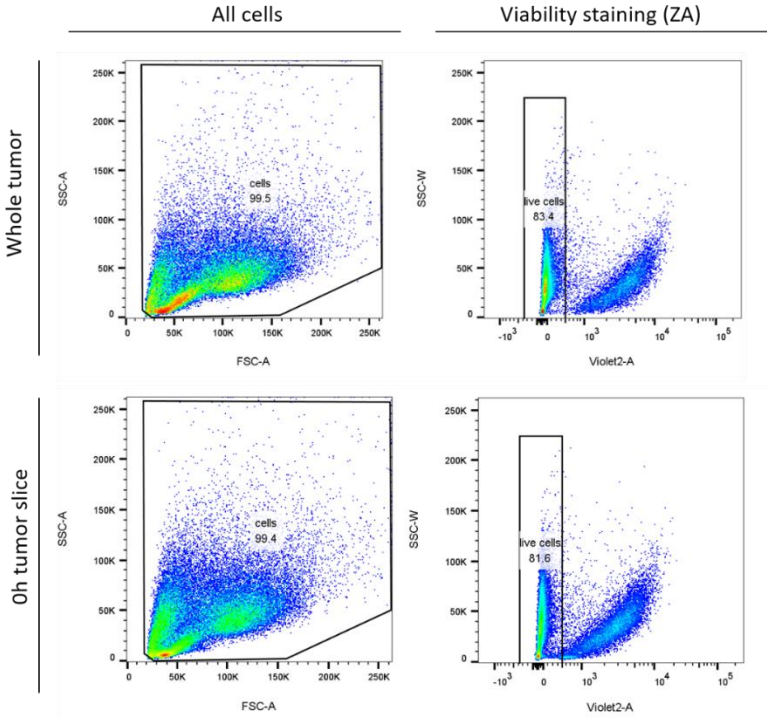


Figure S 2 – FACS histograms for viability staining experiment. Single cell suspensions of unsliced tumor (whole tumor) and a 0h tumor slice were prepared following the approach described above. Cells were staining with Zombie Aqua to assess viability and effect of slicing on cell viability. Unsliced tumor and 0h slice show similar viability, around the 82-83% of total cells.

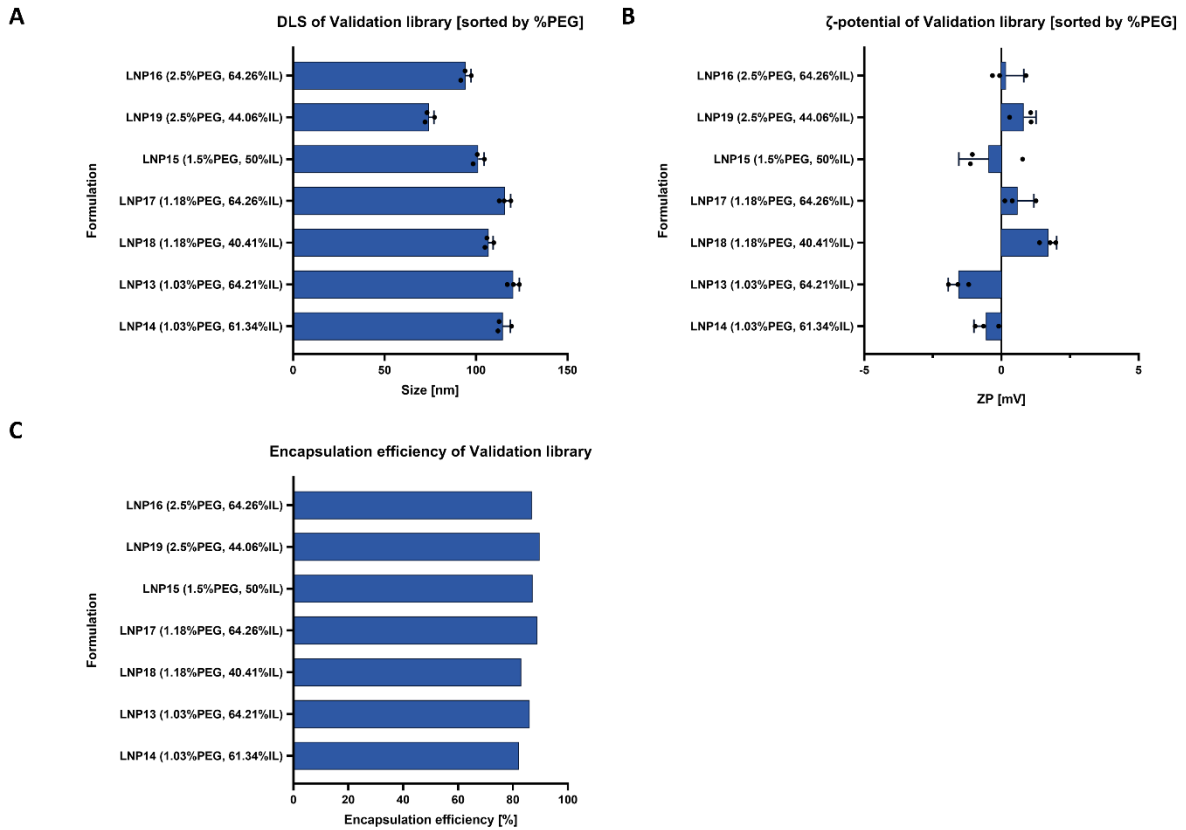


Figure S 3 - Characterization of validation library. (A) Size of Validation LNP formulations, measured by dynamic light scattering. Values represent the mean of three technical measurements. (B) Zetapotential of Validation LNPs, measured by laser Doppler electrophoresis. Values represent the mean of three technical measurements. (C) mRNA encapsulation efficiency of Validation LNP formulations, measured by Ribogreen assay. Values represent the mean of duplicate technical measurements.

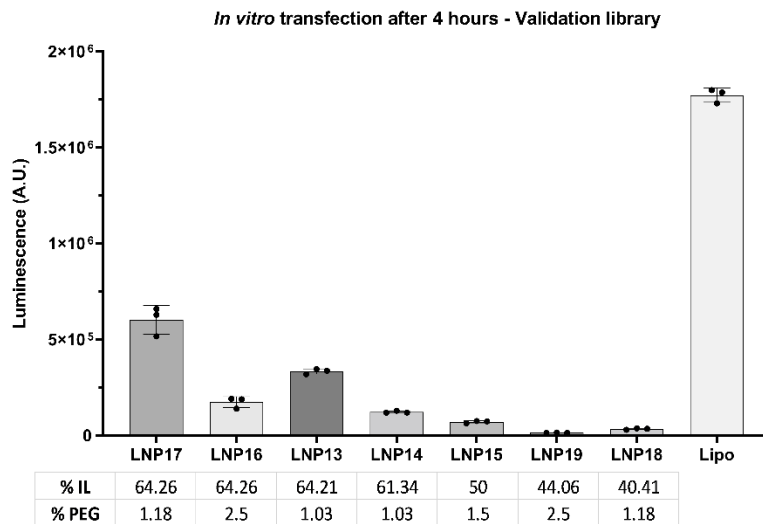


Figure S 4 – 2D *in vitro* transfection of Validation library in MC38 cells measured by luciferase assay after 4 hours. Cells were transfected with LNPs or lipofectamine, equivalent to 200 ng Fluc mRNA per well (10000 cells). Luciferase activity was measured after 4 hours by addition of luciferase reagent to cell lysates, and expressed in luminescence (A.U.). Indicated data points (n=3) represent the mean of duplicate measurements of biological replicates within the same experiment and normalized for background signal.

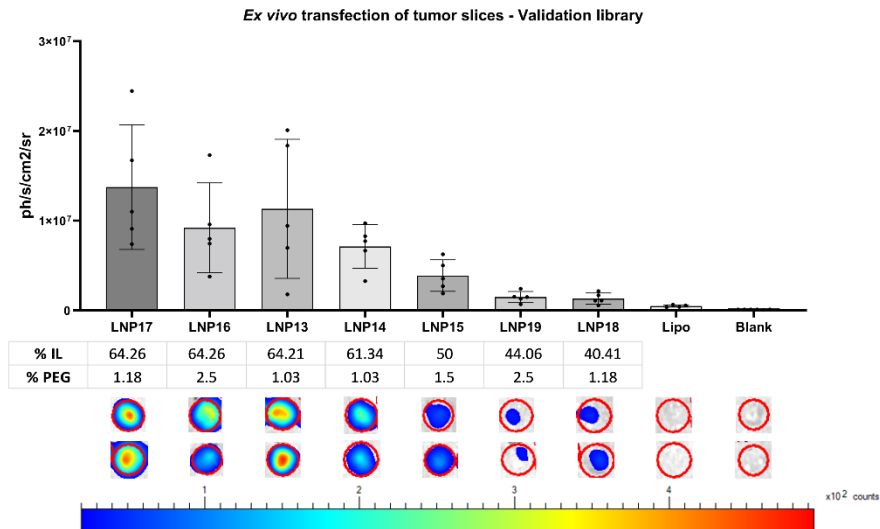


Figure S 5 - Transfection of ex vivo tumor slices with Validation library measured by BLI after 4 hours. Slices were transfected with LNPs or lipofectamine, equivalent to 0.5 μg Fluc mRNA per slice. Transfection efficiency was measured after 4 hours by BLI, after 5 min incubation of the slice in luciferin. The emitted bioluminescence is representative of luciferase activity in transfected slices, expressed in photons emitted per second from the specified area in all directions ($\text{ph/s/cm}^2/\text{sr}$). Indicated data points represent biological replicates ($n=5$) measured in two independent experiments with tumors originating from two distinct mice.

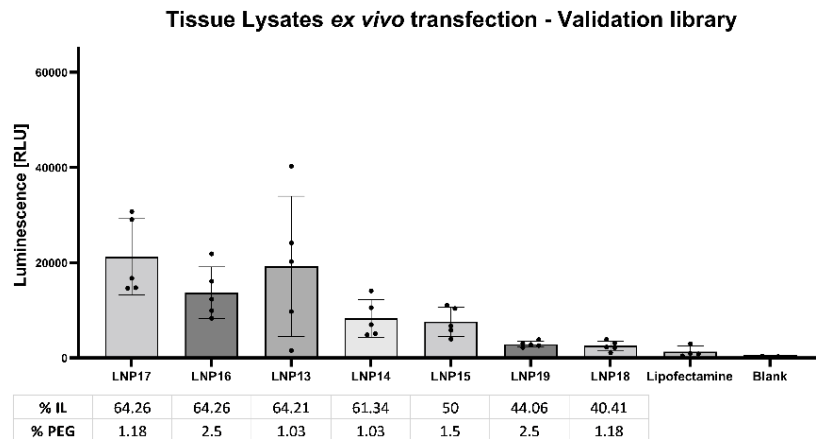


Figure S 6 - Transfection of ex vivo tumor slices with Validation library measured by tissue lysates after 4 hours. Luciferase activity was determined for the tissue lysates obtained from snap-frozen transfected slices, the same samples used for BLI measurements. Luciferase activity was quantified by measuring luminescence emitted upon addition of luciferase reagent and expressed in relative light units (RLU). Indicated data points represent the mean of duplicate measurements for the same biological replicates ($n=5$) used for BLI.